

EFFECTIVE INTERACTION SCALE OF LARGE p_T HADRON PRODUCTION BEYOND LEADING ORDER IN QCD

BY M. A. NOWAK AND M. PRASZAŁOWICZ

Institute of Physics, Jagellonian University, Cracow*

(Received November 23, 1983)

The scale dependence of large p_T hadron production is investigated and analyzed in terms of double moments for $qq \rightarrow qX$ and $qq \rightarrow gX$ partonic subprocesses in the next-to-leading order. Calculated here $qq \rightarrow gX$ cross-section turns out to be small in comparison with quark fragmentation contribution and is shown not to influence the interaction scale extracted according to the fastest apparent convergence criterion.

PACS numbers: 12.35.Eq

1. Introduction

Approaching the end of its first decade, Quantum Chromodynamics (QCD) is still the most promising candidate for the correct theory of the strong interactions (for a review see for example Ref. [1]). The poor understanding of non-perturbative large distance effects strongly urges proving the validity of the theory in short distance domain, which is expected to be simpler and tractable when using perturbative techniques. However, the predictive power of the perturbative QCD is weakened by ambiguities arising from truncation of the perturbative expansion. Such a truncation causes dependence of predictions upon the choice of the scale parameter which has major consequences when performing precise experimental tests of the theory.

In this work we study such a scale dependence on the example of $qq \rightarrow qX$ and $qq \rightarrow gX$ contribution to one hadron inclusive large transverse momentum production. We examine how the value of μ^2 (as extracted from $qq \rightarrow qX$ subprocess by [2]) changes when $qq \rightarrow gX$ contribution is added. We do not analyze high p_T experimental data because our calculations are not renormalization group invariant and are valid only in the large x_T region where the experimental evidence is rather poor [3].

It turns out that $qq \rightarrow gX$ contribution is small as compared with $qq \rightarrow qX$ and does not affect the scale extracted in Ref. [2]. The reason is that $qq \rightarrow qX$ admits $q \rightarrow q$ collinear transitions which are described by P_{qq} Altarelli-Parisi probabilities [4] being $()_+$ distribu-

* Address: Instytut Fizyki UJ, Reymonta 4, 30-059 Kraków, Poland.

tions. Moreover, $qq \rightarrow qX$ contains large virtual corrections to the Born term not present in the $qq \rightarrow gX$ case. From our analysis it is clear that the same subprocesses can give different answers for the "best" scale (if fastest apparent convergence (FAC) criterion [5] is adopted) for different observables like one hadron inclusive production, jet cross-section or unaccompanied particle production.

The work is organized as follows. In Section 2 we sketch the overall procedure of calculating next-to-leading effects on the basis of calculated here $qq \rightarrow gX$ contribution to $pp \rightarrow \pi X$ reaction. Numerical results are presented in Section 3 and Section 4 contains discussion of the results, conclusions and summary. Appendix displays long analytical formulae.

2. Operational procedure

In order to calculate all next-to-leading corrections to large p_T one hadron inclusive production in hadronic collisions we have to take into account the following effects not present at the leading log level:

- two-loop corrections to the effective strong coupling constant,
- two-loop corrections to scaling violation of both singlet and nonsinglet structure (fragmentation) functions
- higher order (α^3) corrections to Born scattering cross section.

The first two problems have been already solved [6–8]. However, the full analysis of the third effect is still lacking (despite the results of Refs. [2, 9–11]) because of the complexity of calculations.

The twist-2 prediction for large p_T hadron-hadron scattering, including all higher order effects mentioned above can be written in the following form:

$$\frac{d\sigma^{h_1 h_2 \rightarrow h_3}(\tau_1, \tau_2, s)}{d\tau_1 d\tau_2} = \sum_{c_1 c_2 c_3} \int_0^1 dz_1 dz_2 dz_3 d\hat{\tau}_1 d\hat{\tau}_2 \delta(\tau_1 - \hat{\tau}_1 z_2 z_3) \delta(\tau_2 - \hat{\tau}_2 z_1 z_3) \\ F_{c_1/h_1}(z_1, \mu^2) \bar{F}_{c_2/h_2}(z_2, \mu^2) \frac{d\bar{\sigma}^{c_1 c_2 \rightarrow c_3}(\hat{\tau}_1, \hat{\tau}_2, \hat{s}, \mu^2)}{d\hat{\tau}_1 d\hat{\tau}_2} \bar{D}_{h_3/c_3}, \quad (2.1)$$

where $\bar{F}_{c/h}$ ($\bar{D}_{h/c}$) denotes structure (fragmentation) function, the sum runs over all hadronic constituents and kinematics is defined by Fig. 1a, b, ($p_T \equiv k_{1T}$, $\hat{p}_T \equiv \hat{k}_{1T}$), and

$$\tau_1 = -\frac{t}{s}, \quad \tau_2 = -\frac{u}{s}, \quad \hat{\tau}_1 = -\frac{\hat{t}}{\hat{s}}, \quad \hat{\tau}_2 = -\frac{\hat{u}}{\hat{s}}. \quad (2.2)$$

The following relations hold:

$$\tau_1 = z_2 z_3 \hat{\tau}_1, \quad \hat{\tau}_2 = z_1 z_3 \hat{\tau}_2, \quad p_T^2 = z_3 \hat{p}_T^2, \\ E^{-1} d^3 k_1 = \pi s d\tau_1 d\tau_2, \quad \hat{E}^{-1} d^3 \hat{k}_1 = \pi \hat{s} d\hat{\tau}_1 d\hat{\tau}_2, \quad (2.3)$$

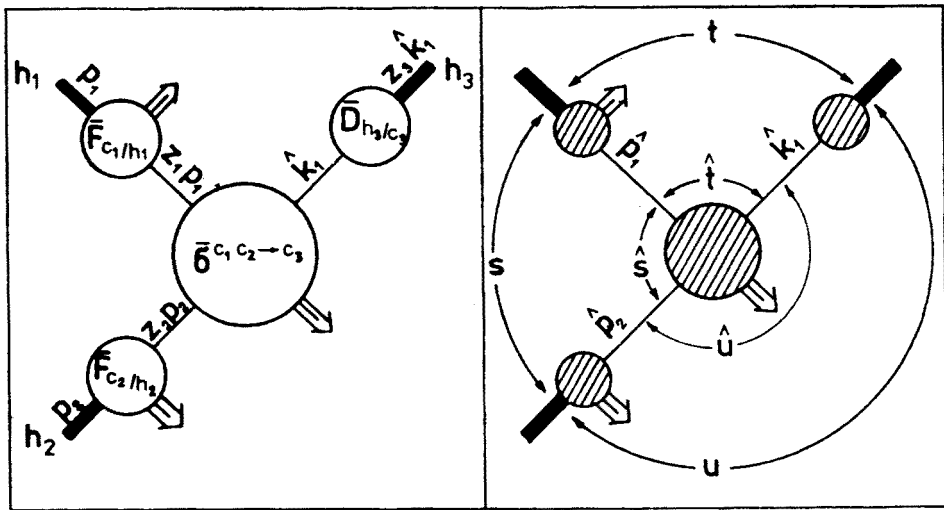


Fig. 1. Kinematics of large p_T one particle inclusive production; a) definition of z_1, z_2, z_3 ; b) definition of s, t, u

where all quantities denoted by a hat ($\hat{}$) refer to partonic subprocesses. It is convenient to introduce the dimensionless functions [2, 12]

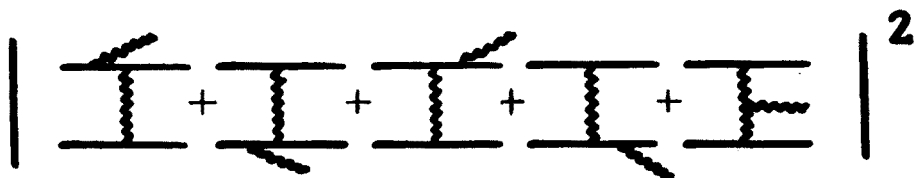
$$E \frac{d^3\sigma}{d^3k_1} = \frac{1}{p_T^4} q\left(\tau_1, \tau_2, \frac{s}{\Lambda^2}\right), \quad \hat{E} \frac{d^3\hat{\sigma}}{d^3\hat{k}_1} = \frac{1}{\hat{p}_T^4} \hat{q}\left(\hat{\tau}_1, \hat{\tau}_2, \frac{\hat{s}}{\mu^2}, \frac{\mu^2}{\Lambda^2}\right). \quad (2.4)$$

Each partonic function has the following perturbative expansion

$$\hat{q}\left(\hat{\tau}_1, \hat{\tau}_2, \frac{\hat{s}}{\mu^2}, \frac{\mu^2}{\Lambda^2}\right) = \left[\frac{\alpha\left(\frac{\mu^2}{\Lambda^2}\right)}{2\pi}\right]^2 \sum_{k=0}^{\infty} \left[\frac{\alpha\left(\frac{\mu^2}{\Lambda^2}\right)}{2\pi}\right]^k \sum_{l=0}^k \hat{q}_l^{(k)}(\hat{\tau}_1, \hat{\tau}_2) \left(\ln \frac{\hat{s}}{\mu^2}\right)^l. \quad (2.5)$$

In this work we use dimensional regularization [13], that is we perform all calculations in $d = 4 - 2\epsilon$ ($\epsilon > 0$) dimensions. Resulting poles in ϵ (UV singularities) are absorbed into renormalization constants together with large finite terms $\ln 4\pi - \gamma_E$ (so called $\overline{\text{MS}}$ -scheme [14]). Next, renormalized quantities are continued to $d = 4 + 2\kappa$ ($\kappa > 0$) dimensions where soft and mass singularities show up as poles in κ . In the full result soft poles cancel and the remaining mass singularities have to be factored out by means of some factorization prescription. In this paper we use the scheme of Ref. [15] (hereafter called CFP scheme).

Let us illustrate how this procedure works in the case of the subprocess $qq \rightarrow gX$. In the order α^3 the full expression for \hat{q} is given by the sum of diagrams depicted in Fig. 2 (we limit ourselves to the non-equal quark flavour case). Because all integrals are UV finite we have performed the calculations right in $d = 4 + 2\kappa$ ($\kappa > 0$) dimensions. Phase space integration has been done according to the method explained in Refs. [12, 16].

Fig. 2. Feynman diagrams for $q_i q_j \rightarrow g q_i q_j$ ($i \neq j$)

The resulting expression for the cross-section reads:

$$\hat{q}(\hat{\tau}_1, \hat{\tau}_2, \dots) = 4\pi^2 \frac{C_F}{n_c} \left[\frac{\alpha(\mu^2)}{2\pi} \right]^3 \left(\frac{\hat{s}\hat{\tau}_1\hat{\tau}_2}{\mu^2} \right)^\kappa \frac{1}{16} \left(\frac{\hat{s}\xi_1}{\mu^2} \right)^\kappa \frac{1}{\kappa} (f_1 + \xi_1^\kappa f_2), \quad (2.6)$$

where

$$\begin{aligned} \xi_1 &= 2\hat{k}_2\hat{k}_3/\hat{s}, \\ f_i(\hat{\tau}_1, \hat{\tau}_2) &= \sum_{k=0} f_i^{(k)}(\hat{\tau}_1, \hat{\tau}_2) \kappa^k, \end{aligned} \quad (2.7)$$

$C_F = \frac{n_c^2 - 1}{2n_c}$, n_c — number of colours. All calculations have been done in Feynman gauge.

The next task is to extract the mass singularities, i.e. to express the formula (2.6) in the form

$$\hat{q} = \hat{q}_{\text{finite}} + \frac{1}{\kappa} \hat{q}_{\text{coll.}} \quad (2.8)$$

According to the CFP prescription $\hat{q}_{\text{coll.}}$ takes a form

$$\hat{q}_{\text{coll.}}(\hat{\tau}_1, \hat{\tau}_2, \dots) = 4\pi \frac{C_F}{n_c} \left[\frac{\alpha(\mu^2)}{2\pi} \right]^3 \left(\frac{\hat{s}\hat{\tau}_1\hat{\tau}_2}{\mu^2} \right)^\kappa \sum_{i=1}^4 P_i(\tilde{z}_i) \sigma_i(\tilde{\tau}_i) J_i, \quad (2.9)$$

where P_i are Altarelli-Parisi probabilities, $\sigma_i = \sigma_i^{(0)} + \kappa \sigma_i^{(1)} + \dots$ — d -dimensional Born cross-sections, J_i — Jacobians originating from δ -functions in (2.1) and from the change of variables. The index i corresponds to four various possibilities of collinear emissions. New variable $\tilde{\tau}_i$ is just $-t/s$ for the hard part of subprocess “ i ” and \tilde{z}_i is a momentum fraction carried by a collinear gluon (see Table I and Appendix).

The factorization theorem is implemented in the following way: first we calculate $\hat{q}(\hat{\tau}_1, \hat{\tau}_2)$ and next subtract $\hat{q}_{\text{coll.}}(\hat{\tau}_1, \hat{\tau}_2)/\kappa$ as given by (2.9). The resulting $\hat{q}_{\text{finite}}(\hat{\tau}_1, \hat{\tau}_2)$ is given (in a $\kappa \rightarrow 0$ limit) by (cf. Eq. (2.5)):

$$\hat{q}_{\text{finite}} = \left[\frac{\alpha(\mu^2)}{2\pi} \right]^3 4\pi^2 \frac{C_F}{n_c} \left(\hat{q}_0^{(1)} + \hat{q}_1^{(1)} \ln \frac{\hat{s}}{\mu^2} \right), \quad (2.10)$$

TABLE I

Collinear emissions in the $q_1 q_j \rightarrow q_1 q_j g$ process

i	1	2	3	4
CONFIGURATION				
$\tilde{\tau}_i$	$\hat{\tau}_1$	$\hat{\tau}_2$	$\hat{\tau}_2/(\hat{\tau}_1 + \hat{\tau}_2)$	$\hat{\tau}_1/(\hat{\tau}_1 + \hat{\tau}_2)$
\tilde{z}_i	$\frac{\hat{\tau}_2}{1 - \hat{\tau}_1}$	$\frac{\hat{\tau}_1}{1 - \hat{\tau}_2}$	$\hat{\tau}_1 + \hat{\tau}_2$	$\hat{\tau}_1 + \hat{\tau}_2$
P_i	$P_{gq}(\tilde{z}_1)$	$P_{gq}(\tilde{z}_2)$	$P_{gq}(\tilde{z}_3)$	$P_{gq}(\tilde{z}_4)$
σ_i	$\frac{d\sigma_{qg}(\tilde{z}_1 \hat{s})}{d\tilde{\tau}_1}$	$\frac{d\sigma_{qg}(\tilde{z}_2 \hat{s})}{d\tilde{\tau}_2}$	$\frac{d\sigma_{qq}(\hat{s})}{d\tilde{\tau}_3}$	$\frac{d\sigma_{qq}(\hat{s})}{d\tilde{\tau}_4}$
J_i	$\tilde{\tau}_1 \tilde{z}_1^2 (1 - \tilde{\tau}_1)^2$	$\tilde{\tau}_2 \tilde{z}_2^2 (1 - \tilde{\tau}_2)^2$	$\tilde{\tau}_3 \tilde{z}_3^3 (1 - \tilde{\tau}_3)^2$	$\tilde{\tau}_4 \tilde{z}_4^3 (1 - \tilde{\tau}_4)^2$
Black dot denotes a collinear emission.				

where

$$\hat{q}_0^{(1)} = \frac{1}{16} [f_1^{(1)} + f_2^{(1)} + f_2^{(0)} \ln \xi_1] + \sum_{i=1}^4 P_i J_i (\sigma_i^{(0)} \ln \xi_1 - \sigma_i^{(1)}),$$

$$\hat{q}_1^{(1)} = \sum_{i=1}^4 P_i J_i \sigma_i^{(0)}. \quad (2.11)$$

Note that for $qq \rightarrow gX$ subprocess $\hat{q}_0^{(0)} = 0$. The formulae for $\hat{q}_0^{(1)}$ and $\hat{q}_1^{(1)}$ are given in the Appendix.

For the purpose of numerical analysis it is convenient to rewrite the above results in terms of single and double moments, defined as follows:

$$g(m, n) = \int_0^1 dx x^{n-1} \int_0^1 dy y^{m-1} \theta(1-x-y) g(x, y),$$

$$g(n) = \int_0^1 dx x^{n-1} g(x). \quad (2.12)$$

Exploiting the relations (2.3) and taking the moments at fixed CM energy of colliding hadrons we can present the formula (2.5) in a simple form:

$$\varrho\left(m, n; \frac{s}{\Lambda^2}\right) = \sum_{ijk} F_{i/h_1}(n+1; \mu^2) F_{j/h_2}(m+1; \mu^2) \times \hat{\varrho}_{finite}^{ijk}(m, n, sf_{ij}(\mu^2), \mu^2) D_{h_3/k}(m+n+3; \mu^2), \quad (2.13)$$

where the sum runs over all possible initial and final partonic states and functions $f_{ij}(n, m; \mu^2)$ are given by [2]

$$\ln f_{ij}(m, n; \mu^2) = \frac{d}{dn} \ln F_{i/h_1}(n+1; \mu^2) + \frac{d}{dm} \ln F_{j/h_2}(m+1; \mu^2). \quad (2.14)$$

In the case of $qq \rightarrow \text{anything}$ process, which is under consideration, the above formula takes the form ($\hat{\varrho} = \hat{\varrho}^{qqq} + \hat{\varrho}^{qqg}$):

$$\varrho(m, n; \dots) = \varrho_B(m, n; \mu^2) \cdot \left[1 + \frac{\alpha(\mu^2)}{2\pi} R_q \left(m, n; \frac{sf(\mu^2)}{\mu^2}, \mu^2 \right) + \frac{\alpha(\mu^2)}{2\pi} R_g \left(m, n; \frac{sf(\mu^2)}{\mu^2}, \mu^2 \right) \frac{D_{h_3/g}^{exp}(m+n+3; \mu^2)}{D_{h_3/q}^{exp}(m+n+3; \mu^2)} \right], \quad (2.15)$$

where the Born cross-section is equal

$$\hat{\varrho}_B(m, n; \mu^2) = \frac{4\pi C_F}{n_c} \left[\frac{\alpha(\mu^2)}{2\pi} \right]^2 F_{q/h_1}^{exp}(n+1; \mu^2) F_{q/h_2}^{exp}(m+1; \mu^2) \times \hat{\varrho}_B(m, n) D_{h_3/q}^{exp}(m+n+3; \mu^2) \quad (2.16)$$

and

$$R_g = \frac{1}{\hat{\varrho}_B} \left[(\hat{\varrho}_0^{(1)})_g + (\hat{\varrho}_1^{(1)})_g \ln \frac{sf(\mu^2)}{\mu^2} \right] = r_g^0 + r_g^1 \ln \frac{sf(\mu^2)}{\mu^2},$$

$$R_q = r_q^0 + r_q^1 \ln \frac{sf(\mu^2)}{\mu^2}, \quad (2.17)$$

$$\hat{\varrho}_B(m, n) = B(m, n+2) + B(m, n+4),$$

$$B(k, l) - \text{Euler beta function.} \quad (2.18)$$

R_q can be found in Ref. [2].

The correction R_q was first calculated by Ellis et al. [9] and Słomiński [2], and R_g is just our result (2.10) divided by the moments of $qq \rightarrow qq$ Born cross-section. Note that both corrections depend on the same function $f(\mu)^2$, involving only incoming non-singlet quark structure functions. This pleasant feature is characteristic only for the moments taken at fixed energy \sqrt{s} .

Before we proceed to the numerical analysis, let us make a few comments concerning the procedure for the choice of the interaction scale. The equivalence of various choices of the interaction scale in leading log formulae forces us to go beyond the lowest order, where corrections have explicit scale dependence [17]. The subleading level, however, is plagued by the problem of ambiguities. They are caused by the application of two procedures removing singularities from the theory, i.e. renormalization and factorization. Perturbative QCD allows us to express the physical quantities, measured at large scales, as series in strong coupling constant $\alpha(\mu^2)$ where μ^2 is a renormalization point. In practice, however, we can compute only a few first terms of this expansion and we have to approximate the observable in question by a truncated and therefore parameter-dependent series. Because the value of the expansion QCD parameter $\alpha(\mu^2)/2\pi$ is rather large (10^{-1}) and some already calculated (for a review see Ref. [1]) approximants exhibit pathological behaviour (correction term is about 200–300% of the lowest order result) the problem of finding the best expansion parameter is crucial from both theoretical and phenomenological viewpoints.

The way of solving the renormalization ambiguity is to find a universal criterion for choosing the value of the scale μ^2 . Different approaches have been proposed: universal momentum subtraction scheme (MOM), Ref. [18], fastest apparent convergence criterion (FAC), Ref. [5] and the principle of minimal sensitivity (PMS), Ref. [19]. The MOM scheme consists in prescribing the values of the one particle irreducible Green functions at some fixed configuration of external momenta p_i with $p_i^2 = -\mu_{\text{MOM}}^2$. The scale μ_{MOM}^2 corresponds to a typical momentum flow through the diagram, but is not defined precisely. Calculations in this scheme are considerably more difficult than in MS, $\overline{\text{MS}}$ renormalization schemes. Moreover, this scheme is strongly gauge dependent — for example in the physical, axial gauge it leads to large corrections [20]. For the above reasons we proceed to considering FAC and PMS to say nothing more of MOM.

FAC criterion chooses the scheme in which the higher order corrections have the least effect on the value of the prediction. A stricter version fixes the scheme by requiring that all known coefficients vanish except the first order term. PMS assumes that the best approximation is the one which is stationary under variation of unphysical parameters, because the true solution is independent of these parameters. It is impossible to prove which criterion is better. In our opinion, PMS is by all means more plausible from the physical point of view, because it is more in the spirit of the renormalization group. In practical QCD applications, however, the PMS approach is almost identical with the FAC [21, 22]. Because in processes involving factorization practical application of the PMS is rather cumbersome [23] we use in Section 3 the stricter FAC version.

3. Numerical results

We begin our analysis by an investigation of the moments of $R_g(m, n)$ in the spirit of Ref. [2]. After applying FAC criterion to R_g alone and imposing

$$\mu^2 = \eta(m, n) \cdot f(m, n; \mu^2) \cdot s \quad (3.1)$$

we can easily find the value of $\ln \eta = (\hat{\varrho}_0^{(1)})_g / (\hat{\varrho}_1^{(1)})_g$ for which $R_g(m, n) = 0$. In Fig. 3 we plot $\ln \eta$ as a function of $z = \frac{n-m}{n+m}$ and $N = n+m$. These variables have the following physical meaning [2]: z corresponds to $\cos \theta_{CM}$ and N to $2E/\sqrt{s}$ (where $\theta_{CM} = \angle(k_1 p_1)$ and E is gluon energy). We see that $\ln \eta(z, N)$ depends rather weakly on z , also the changes

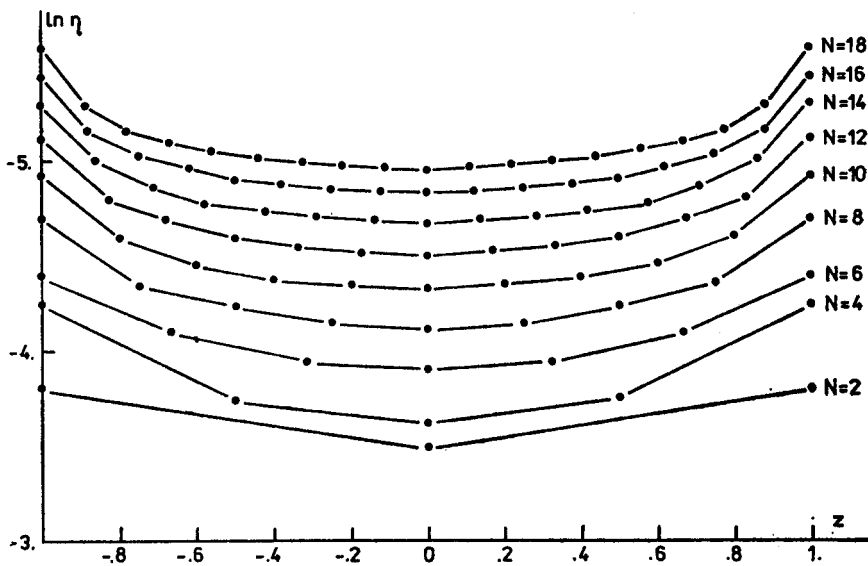


Fig. 3. $\ln \eta$ extracted from Eq. (3.1) as a function of N and z

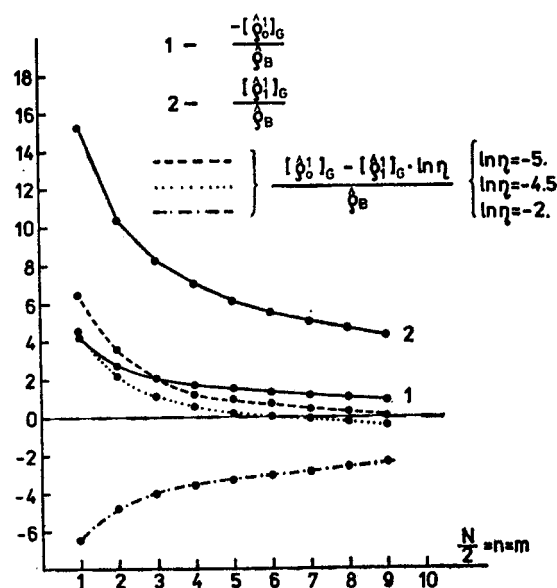


Fig. 4. Diagonal moment of the correction $R_g, r_g^1, -r_g^0$ for various choices of η

with N are not too strong. Therefore we can choose one universal η (N - and z -independent) for which $R_g(m, n) \approx 0$ for wide range of m and n .

As seen from Fig. 3 the negative function $(\hat{\rho}_0^{(1)})_g$ is $4 \div 5$ times larger than the positive function $(\hat{\rho}_0^{(1)})_g$. The same relation can be noticed in Fig. 4 where the full correction R_g together with $-r_g^0$ and r_g^1 (see Eq. (2.17)) is plotted versus $N/2$ for diagonal moments $n = m$ ($z = 0$). One can see from Fig. 4 that the best choice for η is

$$\eta \approx e^{-4.5} \approx 0.01, \quad (3.2)$$

whereas minimization of R_q alone [2] gives $\eta \approx 0.139$.

In Fig. 5 we plot the moments of $R_g(z, N)$ for the naive choice $\ln \eta = 0$ and for $\ln \eta = -4.5$. One can see that for $\eta = e^{-4.5}$ $R_g(z, N)$ is indeed almost 0 for $n, m = 1 \div 18$.

The correction $\frac{\alpha}{2\pi} R_g D_g^{\text{exp}} / D_q^{\text{exp}}$ is depicted in Fig. 6¹. One can see that even for the naive choice of the scale ($\eta = 1$) this correction is only about 10–40% of the Born term

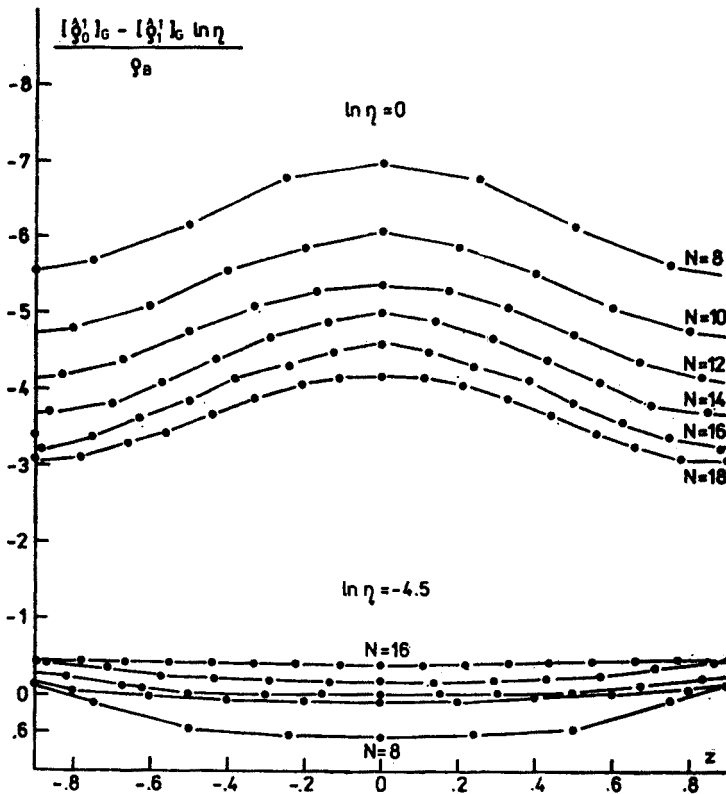


Fig. 5. Double moments of R_g for $\ln \eta = 1$ and $= \ln \eta - 4.5$

¹ For D_g^{exp} and D_q^{exp} we take $q \rightarrow \pi^0$ and $g \rightarrow \pi^0$ fragmentation functions from Ref. [24].

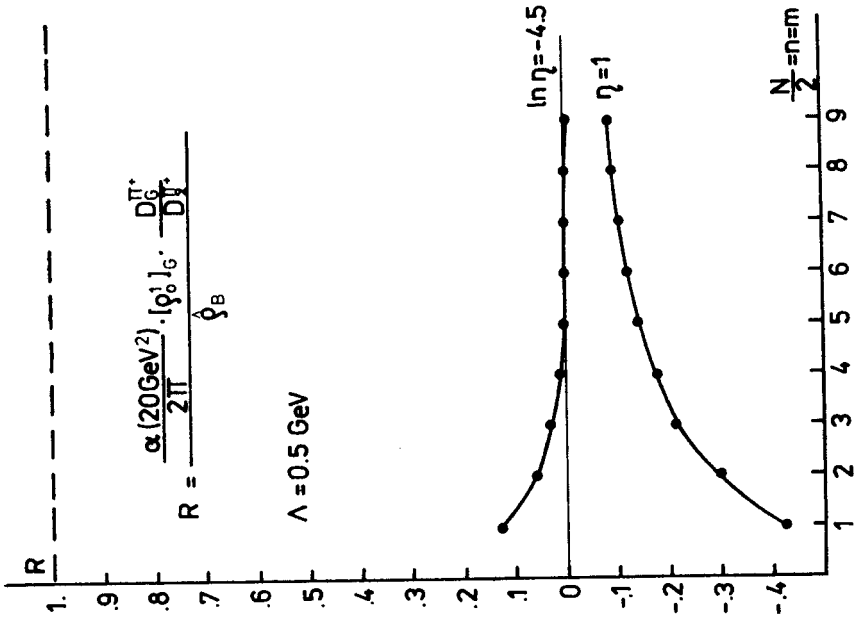


Fig. 6

Fig. 6. Diagonal moments of $\alpha/2\pi R_g \cdot D_g^{\text{exp}}/D_q^{\text{exp}}$ for $\ln \eta = 1$ and $\ln \eta = -4.5$

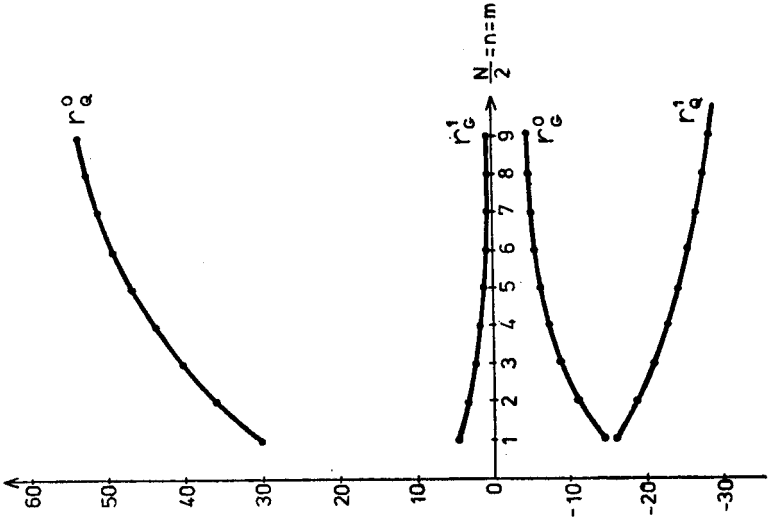


Fig. 7

Fig. 7. Diagonal moments of gluon correction r_g^0 , r_g^1 and quark correction r_q^1 taken from Ref. [2]

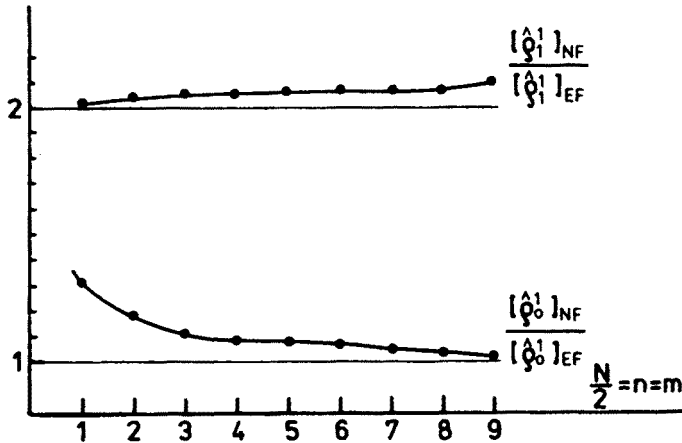


Fig. 8. Effects of equal flavours (EF) antisymmetrization for diagonal moments of gluonic functions $\hat{q}_1^{(1)}, \hat{q}_0^{(1)}$

unlike the R_q case where $\frac{\alpha}{2\pi} R_q(\eta = 1) = 1 \div 3$. Therefore we can conclude that gluon fragmentation in $q + q$ scattering is not important in large p_T one particle inclusive production and has no influence on the overall interaction scale.

In Fig. 7 we display functions r_g^0, r_g^1 , and r_q^0, r_q^1 from Ref. [2].

Until now we have been discussing only non-equal flavour (NF) contribution to the $qq \rightarrow gX$ process. We have also calculated the equal flavour (EF) cross-section. The moments of the ratios NF/EF for $(\hat{q}_0^{(1)})_g$ and $(\hat{q}_1^{(1)})_g$ are depicted in Fig. 8. Note that $(\hat{q}_1^{(1)})_g^{EF}$ is completely determined by the factorization prescription alone. As seen from Fig. 8, $(\hat{q}_0^{(1)})_g^{NF} \approx (\hat{q}_0^{(1)})_g^{EF}$. The addition of EF contribution does not change substantially the scale η ($\ln \eta_{EF} \approx 1.5 \ln \eta_{NF}$, [25]).

We have also investigated the importance of the 3-gluon coupling by plotting the magnitude of $qq \rightarrow gX$ cross-section for $C_A = 0$. This is shown in Fig. 9. We see that more than half of the cross-section comes from the non-abelian 3g coupling.

Now, taking into account both corrections we can find η_{eff} by solving the equation:

$$R_q(m, n; \eta) + R_g(m, n; \eta)W(m, n) = 0, \quad (3.3)$$

where

$$W(m, n) = \frac{D_g^{exp}(m+n+3)}{D_q^{exp}(m+n+3)}. \quad (3.4)$$

In Fig. 10 we plot $\ln \eta_{eff}$ for $W(m, n)$ given by (3.4) also for sample $W = 1, 0.1$. One can see that with increasing N $\ln \eta_{eff} \rightarrow -2$, that is the value obtained for $qq \rightarrow qX$ alone. When we know η_{eff} we can find the effective scale of interactions Q_{eff}^2 , which is the solution of

$$Q_{eff}^2 = s \cdot \eta_{eff} \cdot f(m, n; Q_{eff}^2). \quad (3.5)$$

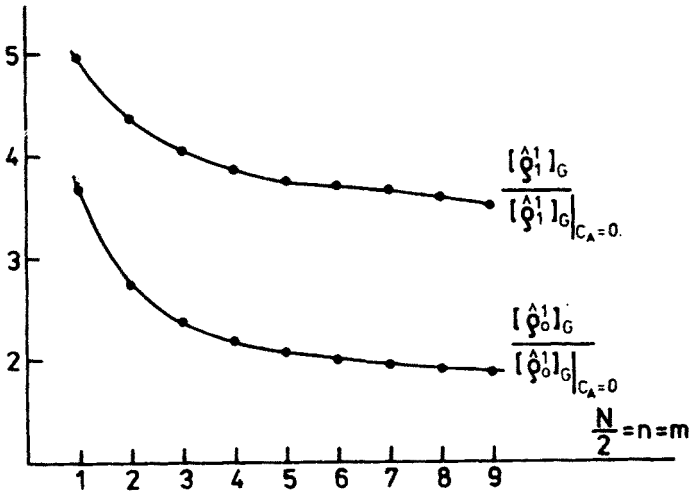


Fig. 9. Effects of triple gluon coupling for diagonal moments of gluonic functions $\hat{\varphi}_1^{(1)}, \hat{\varphi}_0^{(1)}$

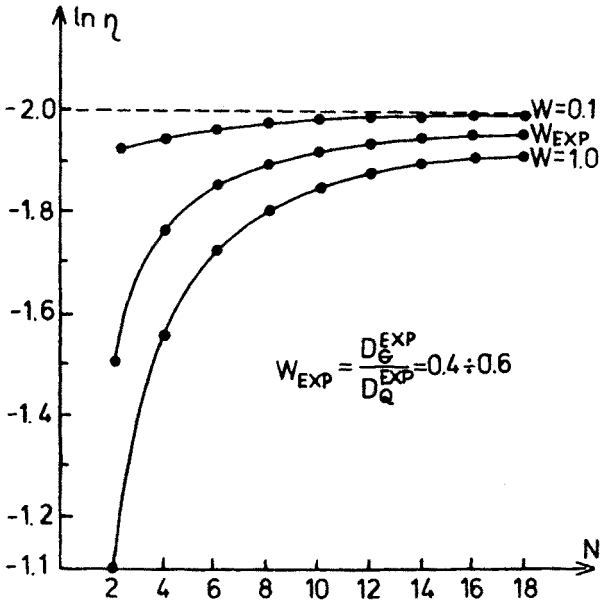


Fig. 10. Diagonal moments of $\ln \eta_{\text{eff}}$ (see text) for various choices of $W = D_G^{\text{EXP}}/D_Q^{\text{EXP}}$

We solve this equation for the sample input $Q_0^2 = 20 \text{ GeV}$, $\Lambda = 500 \text{ MeV}$, $\sqrt{s} = 63 \text{ GeV}$ and we plot the results for $\eta_{\text{eff}}, \eta_g, \eta_q$ in Fig. 11. The scale Q_{eff}^2 comprises all NTL effects. Such a procedure of extracting the scale, although cumbersome, is necessary because of the complexity of the process in question. In lepton-hadron processes, elementary ‘probes’ like virtuality of photon in deep inelastic scattering or Drell-Yan pair momentum distribution inform us about the scale of partonic interactions. On the contrary, in hadronic proc-

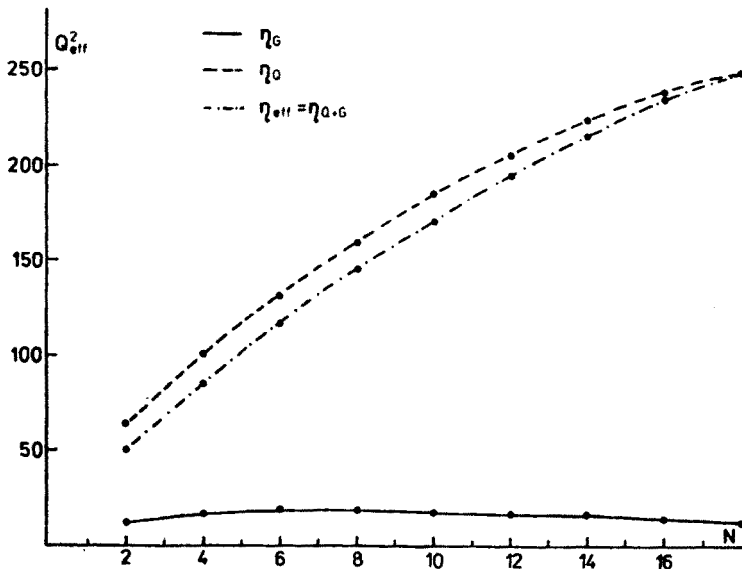


Fig. 11. Q_{eff}^2 (see Eq. (3.5)) for different η (see Eq. (4.2))

esses all scales of interactions are a priori equivalent. The naive choice of scale (\hat{s} , p_T^2 , $2\hat{s}\hat{t}\hat{u}/(\hat{s}^2 + \hat{t}^2 + \hat{u}^2)$) leads to huge corrections. Hence the only way is the choice of the scale a posteriori, applying some universal hypothesis about convergence of perturbative expansion like FAC.

4. Discussion and summary

The aim of this work was to study the choice of the effective scale of large p_T hadron production in hadronic collisions by means of the FAC criterion. Single π^0 production in pp interaction was taken as an example and the interplay of two partonic subprocesses

$$q + q \rightarrow q + x; \quad q \rightarrow \pi^0, \quad (4.1a)$$

$$q + q \rightarrow g + x; \quad g \rightarrow \pi^0 \quad (4.1b)$$

was examined.

Our first observation is that the contribution of (4.1b) is small in comparison with (4.1a) and therefore it does not affect the scale parameter extracted from (4.1a) alone. However, the scale chosen on the basis of (4.1b) alone is very much different from $Q_{\text{eff}}^2 = \eta_{\text{eff}} \cdot f \cdot s$ (see Eqs. (3.1) and (3.3)) and therefore one has to be very careful in making definite statements on the basis of only one partonic subprocess.

Let us illustrate this in some detail. The fixed s moments of the cross-section for $pp \rightarrow \pi^0 X$ are given by Eq. (2.15). Now FAC says that in order to find a proper scale (i.e. η , see Eq. (3.1)) one should solve Eq. (3.3).

First let us observe that (see Fig. 7)

$$\begin{aligned} r_q^0 > 0, r_q^1 < 0; \quad R_q = 0 \Rightarrow r_q^0 = -2r_q^1 \Rightarrow \eta_q \simeq 0.139, \\ r_g^0 < 0, r_g^1 > 0; \quad R_g = 0 \Rightarrow r_g^0 = -4.5r_g^1 = \eta_g \simeq 0.01. \end{aligned} \quad (4.2)$$

The signs and magnitudes of r_a^i corrections can be understood in the following way. In the $q+q \rightarrow q+X$ subprocess r_q^1 is dominated by the moments of $P_{qq}(x)$ giving large and negative numbers (due to $(\)_+$ distributions) whereas r_g^1 includes only non-diagonal probability $P_{gq}(n)$, which is small, positive and decreases with growing n .

The negative value of r_g^0 is caused, as we think, by factorization of poles in κ . Three particle phase-space contains the factor ξ_1^κ which, when expanded in κ , gives contribution to r_g^0 (see Eq. (2.11)):

$$r_g^0 = r_g^1 \ln \xi_1 + \text{other terms.} \quad (4.3)$$

Since $\xi_1 \leq 1$, the first term is negative, however we cannot give an explanation why *other terms* do not change the sign of r_g^0 . Note that in case of r_q^0 the term $r_q^1 \ln \xi_1$ is large and positive, and moreover r_q^0 is enhanced by *other terms* — large positive constants originating from the virtual diagrams [2].

Because the influence of $qq \rightarrow gX$ scattering on the overall value of η_{eff} is rather weak (Fig. 11), $\eta_{\text{eff}} \approx \eta_q$ for a wide range of the parameter $W = D_g^{\text{exp}}(n, Q^2)/D_q^{\text{exp}}(n, Q^2)$.

Let us stress that the results quoted above are unfortunately process-dependent; i.e. if we define our observable in a different way (with some energy-angular cut-off for a jet cross-section or for direct photon production for example) then the result for η can be substantially different. Suppose that, like in the direct photon production [12], we require that a photon is not accompanied in a cone of a half-opening angle 2δ . In that case the integration over the 3-particle phase-space (with $o(\delta^2)$ accuracy) gives²

$$\bar{R}_\gamma = r_\gamma^0 + \left(\frac{1}{\eta}\right)^\kappa \left[(1-\delta^{2\kappa}) r_\gamma^f \frac{1}{\kappa} + r_\gamma^i \frac{1}{\kappa} \right], \quad (4.4)$$

where \bar{R}_γ still contains poles in κ which have to be factored out by means of some factorization prescription. For $\delta = 0$ (i.e. for accompanied and unaccompanied photons) the finite answer for R_γ reads

$$R_{\gamma\mathbf{I}}^0 = r_\gamma^0 + (r_\gamma^f + r_\gamma^i) \ln \frac{1}{\eta}, \quad (4.5)$$

whereas, if we keep $\delta \neq 0$ (unaccompanied photons)

$$R_\gamma^\delta = r_\gamma^0 - r_\gamma^f \ln \delta^2 + r_\gamma^i \ln \frac{1}{\eta}, \quad (4.6)$$

where r_γ^f, r_γ^i correspond to final and initial state collinear emissions respectively. It is easily seen that η extracted from $R_\gamma^\delta = 0$ and $R_\gamma^0 = 0$ are different.

² Strictly speaking in Eq. (4.4) $\delta^2 = (\text{angular cut-off})^2 * h(n, m)$, where h is a calculable function.

The same argument can be applied to the jet cross-sections, one should however remember that in this case there is one more integration which leads to $\log E$ terms, where E is an energy cut-off [10]. So we arrive at the conclusion that for different observables the same partonic subprocesses may account for different scales in the FAC approach.

Let us note at the end that moment analysis favours some regions of phase-space and therefore the direct analysis of the cross-sections themselves would be very interesting, especially their μ^2 dependence [26].

Finally let us stress that careful analysis of experimental data at hand is only reliable when all contributions to renormalization group invariant cross-section are simultaneously taken into account. In case of large p_T inclusive hadron production this formidable program is unlikely to be realized because of the complexity of calculations. However, it can be carried out for simpler processes like direct photon production or Drell-Yan process. We think that this still remains an appealing problem.

The authors are indebted to Dr. Wojtek Słomiński for many discussions and Dr. Wojtek Furmański for bringing their attention to the problem investigated in this paper.

APPENDIX

1. Functions $(\hat{q}_0^{(1)})_g$, $(\hat{q}_1^{(1)})_g$

The function $(\hat{q}_0^{(1)})_g$ has the following form:

$$(\hat{q}_0^{(1)})_g = \sum_{i=0}^3 \sum_{j=0}^4 A_{ij} \tilde{z}_1^i \tilde{\tau}_1^j + \sum_{i=1}^4 \sum_{j=1}^4 B_{ij} \tilde{z}_3^i \tilde{\tau}_3^j + (\hat{\tau}_1 \leftrightarrow \hat{\tau}_2).$$

The coefficients A_{ij} , B_{ij} are given in Tables II, III respectively. We use the following notation

$$\begin{aligned} l &= \ln \tilde{z}_k, & t &= \ln \tilde{\tau}_k, \\ l &= \ln(1 - \tilde{z}_k), & \bar{t} &= \ln(1 - \tilde{\tau}_k), \\ x &= l + t, \end{aligned}$$

where $k = \begin{cases} 1 & \text{for } A_{ij}, \\ 3 & \text{for } B_{ij}. \end{cases}$

The function $(\hat{q}_1^{(1)})_g$ is given by

$$\begin{aligned} (\hat{q}_1^{(1)})_g &= [C_F \tilde{\tau}_1^2 + C_A(1 - \tilde{\tau}_1)] [1 + (1 - \tilde{\tau}_1)^2] [1 + (1 - \tilde{z}_1)^2] \\ &\quad + C_F [(1 - \tilde{\tau}_3)^2 + (1 - \tilde{\tau}_3)^4] [1 + (1 - \tilde{z}_3)^2] \tilde{z}_3^2 + (\hat{\tau}_1 \leftrightarrow \hat{\tau}_2). \end{aligned}$$

2. Born cross-sections in $d = 4 + 2\kappa$ dimensions

$$\begin{aligned} \frac{d\sigma(s)}{dx} [q_i q_j \rightarrow q_i q_j] &= \frac{C_F}{n_c} \mathcal{M} \left(\frac{1 + (1-x)^2}{x^2} + \kappa \right), \\ \frac{d\sigma(s)}{dx} [qg \rightarrow qg] &= \frac{1}{n_c} \mathcal{M} \left(\frac{C_F}{1-x} + \frac{C_A}{x^2} \right) (1 + (1-x)^2 + \kappa x^2), \end{aligned}$$

TABLE II

Coefficients A_{ij}

$i \backslash j$	0	1	2	3	4
0	$C_A 4(x + \bar{i})$	$C_A(-6x - 12\bar{i} - 2\bar{i}) + C_F(8\bar{i} + 8\bar{i})$	$C_A(4x + 12\bar{i} + 4\bar{i}) + C_F(-8\bar{i} - 16\bar{i})$	$C_A(-x - 5\bar{i} - 2\bar{i}) + C_F(2\bar{i} + 10\bar{i})$	$C_A(\bar{i} + \bar{i}) - C_F 4\bar{i}$
1	$-C_A(6x + 2\bar{i})$	$C_A(12x + 7\bar{i} - \bar{i}) - C_F 8\bar{i}$	$C_A(-8x - \frac{1}{2}\bar{i} + \frac{3}{2}\bar{i} + 1) + C_F(8\bar{i} - 2)$	$C_A(2x + \frac{5}{2}\bar{i} - \frac{1}{2}\bar{i} - 1) + C_F(-4\bar{i} + 3)$	$C_F(-2\bar{i} + 2\bar{i})$
2	$C_A(4x + 2)$	$C_A(-10x + \bar{i} - 5) + C_F(4\bar{i} + 2)$	$C_A(8x + \bar{i} - \bar{i} + 3) + C_F(-6\bar{i} + 1)$	$C_A(-2x - \bar{i}) + C_F(2\bar{i} + 2\bar{i} - 5)$	$C_F(\bar{i} + 1 - \bar{i})$
3	$C_A(-x + \bar{i})$	$C_A(3x - 3\bar{i})$	$C_A(-3x + 3\bar{i})$	$C_A(x - \bar{i})$	0

TABLE III

Coefficients B_{ij}

$i \backslash j$	0	1	2	3	4
1	0	$-C_A 2\bar{i} + C_F 8\bar{i}$	$C_A 4\bar{i} - C_F 8\bar{i}$	0	0
2	0	$C_A(3\bar{i} + 4t) + C_F(-12\bar{i} - 16t + 1)$	$C_A(-7\bar{i} - 12t + 4) + C_F(18\bar{i} + 40t - 13)$	$C_A(2\bar{i} + 8t - 8) + C_F(-4\bar{i} - 16t + 24)$	$C_A 4 + C_F(2\bar{i} - 12)$
3	0	$C_A(-\frac{3}{2}\bar{i} - 2t) + C_F(6\bar{i} + 8t)$	$C_A(4\bar{i} + 6t - 2) + C_F(-12\bar{i} - 20t + 6)$	$C_A(-\frac{5}{2}\bar{i} - 4t + 4) + C_F(6\bar{i} + 4t - 12)$	$C_A(\bar{i} - 2) + C_F(-4\bar{i} + 6)$
4	0	0	$C_F(\bar{i} + 2t + 1)$	0	$C_F(1 + 2t + \bar{i})$

where

$$\mathcal{M} = \mu^{-2\kappa} \alpha^2 (\mu^2) \frac{\pi}{s} \left(\frac{s}{4\pi\mu^2} \right)^\kappa \frac{x^\kappa (1-x)^\kappa}{\Gamma(1+\kappa)}$$

and

$$x = -\frac{t}{s}.$$

REFERENCES

- [1] A. J. Buras, Fermilab preprint, Conf-81/61-THY, 1981.
- [2] W. Furmański, W. Słomiński, preprint TPJU-11/81, Cracow 1981.
- [3] P. Darriulat, CERN preprint, CERN-EP/80-16, 1980.
- [4] G. Altarelli, G. Parisi, *Nucl. Phys.* **B126**, 298 (1977).
- [5] G. Grunberg, *Phys. Lett.* **95B**, 70 (1980).
- [6] W. Caswell, *Phys. Rev. Lett.* **33**, 244 (1974).
- [7] D. R. T. Jones, *Nucl. Phys.* **B75**, 531 (1974).
- [8] W. Furmański, R. Petronzio, *Phys. Lett.* **93B**, 437 (1980).

- [9] R. K. Ellis, M. A. Furman, H. E. Haber, I. Hinchliffe, *Nucl. Phys.* **B173**, 397 (1980).
- [10] M. A. Furman, Columbia preprint, CU-TP-183, 1980.
- [11] R. K. Ellis, G. Martinelli, R. Petronzio, *Phys. Lett.* **104B**, 45 (1981); H. Perl, *Z. Phys.* **C17**, 153 (1983).
- [12] M. A. Nowak, M. Praszalowicz, *Z. Phys.* **C17**, 249 (1983).
- [13] G. 't Hooft, M. Veltman, *Nucl. Phys.* **B44**, 189 (1972).
- [14] W. A. Bardeen, A. J. Buras, D. W. Duke, T. Muta, *Phys. Rev.* **D18**, 3998 (1978).
- [15] G. Curci, W. Furmanski, R. Petronzio, *Nucl. Phys.* **B175**, 27 (1980).
- [16] M. A. Nowak, M. Praszalowicz, W. Słomiński, 1983, to be published.
- [17] M. Bacé, *Phys. Lett.* **78B**, 132 (1978).
- [18] W. Celmaster, R. J. Gonsalves, *Phys. Rev.* **D20**, 1420 (1979).
- [19] P. M. Stevenson, *Phys. Lett.* **B100**, 61 (1981).
- [20] W. L. van Neerven, *Z. Phys.* **C14**, 241 (1982).
- [21] D. W. Duke, J. Kimel, *Phys. Rev.* **D25**, 71 (1982).
- [22] M. R. Pennington, *Phys. Rev.* **D26**, 2048 (1982).
- [23] H. D. Politzer, *Nucl. Phys.* **B194**, 492 (1982).
- [24] M. Glück, J. F. Owens, E. Reya, *Phys. Rev.* **D18**, 1501 (1978).
- [25] M. A. Nowak, Ph. D. Thesis, Jagellonian University 1983, unpublished.
- [26] M. A. Nowak, M. Praszalowicz, work in progress.